Performance analysis of a Stirling engine hybrid power system

Pablo Jimenez Zabalaga[a], Luis A. Choque Campero[b], Joseph Adhemar Araoz Ramos[c]

[a] *University Mayor de San Simon, Cochabamba, Bolivia, pabloadolfo24@gmail.com*
[b] *University Mayor de San Simon, Cochabamba, Bolivia, luiscc@kth.se*
[c] *University Mayor de San Simon, Cochabamba, Bolivia, araoz@kth.se*

Abstract:

This article presents the performance analysis related to energy efficiency, economic feasibility and environmental sustainability of a hybrid power system, composed of photovoltaic modules, batteries and a Stirling engine powered by wood pellets. The analysis includes the dynamic start-up and cooling phases of the system, and then compares its performance with a hybrid photovoltaic-diesel-battery system. The first system consists of a 5.45 kW solar array, a 6 kW Stirling engine, a 6.92 kW bi-directional inverter and a 71.28 kWh VRLA gel lead-acid battery bank. The second one is comprised of 3.95 kW PV panels, a 7.1 kW diesel genset, a 4.46 kW bi-directional inverter and a 50.16 kWh VRLA gel lead-acid battery bank. The initial sizing of both systems was based on the demand estimated for a hypothetical case study of electrification for a 102-household rural village in Bolivia called "Tacuaral de Mattos". Both systems were initially optimized in size using the well-known energy optimization software tool, HOMER. However, since the characteristics of the proposed system required a detailed analysis of its dynamics, a dynamic model that complements the HOMER analysis was developed using MATLAB Simulink TM 8.9. Furthermore, due to fluctuations of photovoltaic energy as well as the importance of the battery life cycle, a smart power management was implemented through combined dispatch algorithms. These control algorithms were composed of typical "cycle charging", "load following", "frugal" and "SOC set point" strategies. Additionally, a supervisory controller was designed in order to compensate the energy difference during the warm-up, stand-by and cool-down modes of the Stirling engine and diesel generator. The results showed that PV-diesel-battery system represented a higher-performance option to implement in a rural electrification project compared to a PV-Stirling-battery system. However, the last one showed a better environmental sustainability as it was able to reduce carbon dioxide emissions during its operation (Around 10% savings in CO_2 emissions).

Keywords:

Hybrid power system; Micro-grid; PV panel; Stirling engine; Diesel genset; Lead-acid battery; Bi-directional inverter; Bolivia.

1. Introduction

The role of electricity is essential for the economic and social development in a community [1]. Unfortunately, around one billion people (14% of the world's population) do not have access to electricity. Likewise, many more suffer from a low-quality service, generally in rural areas [2]. Under this consideration, developing countries are making strenuous efforts to sponsor the expansion of electricity generation systems in remote areas. Although fossil fuel generators (especially diesel), are the main source of electricity in many rural communities worldwide, the growing energy demand, the unstable prices of fossil fuels, the depletion of oil resources, as well as the growing concern about greenhouse gas emissions, are incrementing the use of renewable energy sources [3].

In Bolivia, around 44% of the inhabitants of rural areas do not have access to electricity [4]. According to the Electricity and Social Control Authority (Autoridad de Fiscalización y Control Social de Electricidad, AE), the residential sector of the isolated electrical generation systems represented 7.42% (171.88 MW) of the total electric power generated in the country in 2017. In their majority, these systems are composed of fossil fuel generators (97%) and arrays of photovoltaic modules (3%). Additionally, they are also located in the northern and eastern populations of the country; being Beni the department that concentrates most of its users, with 58% of the 163,149 total users of these isolated systems [5].

Bolivian government concern is that diesel is imported by the state-owned Oil and Gas Company of Bolivia (Yacimientos Petrolíferos Fiscales Bolivianos, YPFB) and provided to the operators of the plants of the isolated electrical systems at a subsidized price of 0.16 USD/L, despite the fact that the market cost for import the mentioned fuel is over 1.30 USD/L [6]. For this reason, the Bolivian government has been promoting projects for the hybridization of thermoelectric remote plants in order to reduce the consumption of diesel in electricity generation. The FV-diesel-battery hybrid plants installed in the city of Cobija and in the community of El Espino are examples of this trend [7] [8].

In this context, the following research aimed to evaluate the performance of a completely renewable hybrid system (PV-Stirling-battery system), by considering indicators for energy performance, level of costs, and environmental impact. Furthermore, a PV-diesel-battery system (which is commonly used), was also evaluated and compared with the Stirling based one. Both analyses were developed for the electrification of a rural community in Bolivia named “Tacuaral de Mattos".

1.1. Methodology

This research addresses the performance related to energy efficiency, economic feasibility and environmental sustainability of a PV-Stirling-battery system which is powered by wood pellets under transient warm-up and shut-down periods and compared to a hybrid PV-diesel-battery system. Hence, a process of economic optimization, dynamic modelling, simulation, and final evaluation of performance were carried out; as presented in Fig. 1.

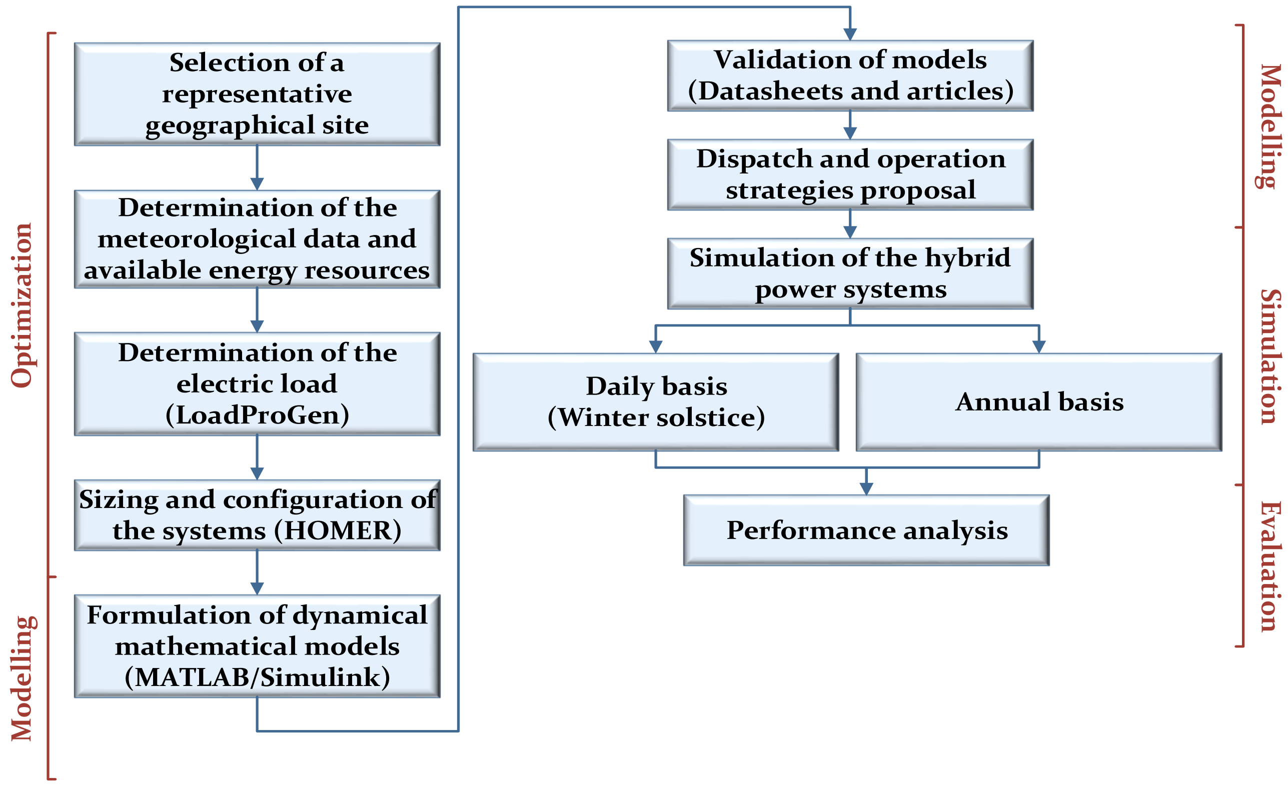

Figure 1. Methodology and general approach of system analysis.

While the meteorological data (Solar insolation and average ambient temperature) were extracted from the Meteonorm software v.7.1.3 [9], the electric demand pattern per minute was obtained through the use of the LoadProGen software [10], in order to use them as inputs from Hybrid Optimization of Multiple Energy Resources Software (HOMER) which led to techno-economically optimized configurations [11]. As for the modelling, dynamic mathematical models were developed for the different studied technologies. These components were implemented using MATLAB Simulink TM 8.9 [12]; the validation process was carried out through experimental data shown in datasheets and scientific articles. Two dispatch strategies were implemented for the simulation: Cycle Charging-Frugal-SOC Setpoint (PV-Stirling-battery system) and Load Following-Frugal (PV-diesel-battery system), including an internal control system used to compensate the energy difference during the start and stop periods of the generators. Finally, the evaluation of the performance of the hybrid generation systems were carried out in terms of the 3-E analysis [13].

2. Economic Optimization

Two models, that consist of solar PV panels, battery bank, bi-directional inverter and generator (diesel genset/Stirling engine), had been implemented in HOMER software. In the following section, the inputs and assumptions of the models such as meteorological data and energy resources for the selected location, load demand for the community, the specification of components and their respective costs are detailed.

2.1. Site selection and energy primary sources

The first choice made within the design process was the selection of the site where the electric generation systems would be implemented. In this specific case, it is assumed that hybrid microgrids should provide electricity to a community in the department of Beni, called “Tacuaral de Mattos” (-14.993,-66.537), which has the largest number of houses without electricity access. Furthermore, it was estimated that it had an average of 102 households and population of 527 inhabitants by the year 2017 [14]. In this way, this decision led to determine the availability of resources such as solar radiation and biomass. Bolivia has high solar radiation, due to its proximity to the Equator line [15]. Moreover, the departments that have the largest amount of available biomass are the ones belonging to the tropical lowlands (Pando, Beni and Santa Cruz) [16]. These facts serve as motivation for the selection of the site because the potential of a Stirling engine powered by biomass.

2.2. Load Characteristics

The aim of the hybrid systems were not only to cover the demand of the households, but also of its two schools, the church, the primary healthcare facility and the streetlight. The load demand details are shown in Table 1. The assumptions regarding appliances, their daily usage and their power consumption were taken from diverse Bolivian literature sources [16] [17] [18].

Table 1. Daily electricity demand in Tacuaral de Mattos community.

Type of Load	*Power*	*Duration*
	Household	
Lighting	3 * 14 W	19:00 – 22:00
Mobile charging	3 * 5 W	19:00 – 21:00
	Each of both schools	
Computer	9 * 50 W	07:30 – 12:30 15:00 – 18:00
Printer	20 W	
Mobile charging	5 * 2 W	
	Church	
Lighting	10 * 26 W	20:00 – 00:00
External Lighting	7 * 30 W	
Speaker	100 W	20:00 – 22:30
	Primary healthcare facility	
Lighting	5 * 26 W	08:00 – 12:00 19:00 – 22:30
External Lighting	30 W	18:30 – 22:30
TV	80 W	07:00 – 12:00
Mobile charging	2 * 2 W	05:00 – 23:00
Small fridge	80 W	Whole day
Computer	50 W	Whole day
	Streetlight	
Streetlight	100 W	19:00 – 06:00

2.3. Configuration

The architecture of both systems was based on the centralized AC bus. This decision was motivated by the modular configuration that allows adapting to the growth of electricity demand in the future, and it was the configuration implemented for the hybrid system of the community of El Espino [19]. Therefore, the configurations of the PV-diesel-battery and PV-Stirling-battery systems are shown in Fig. 2.

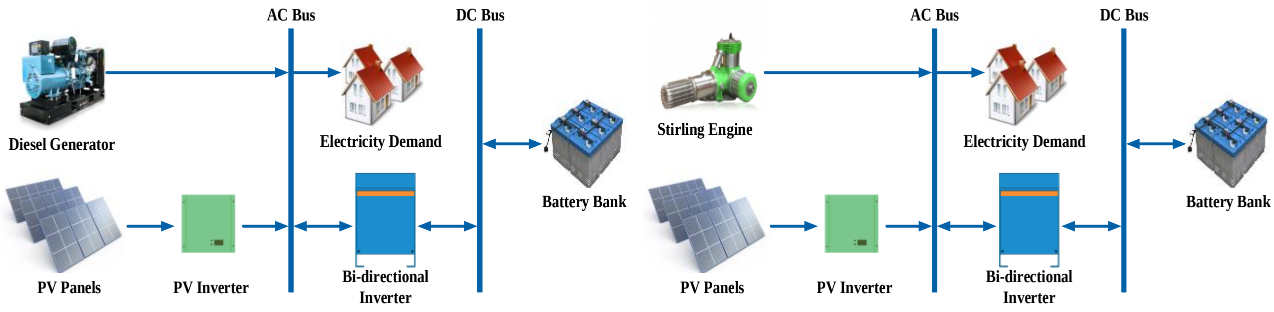

(a) (b)

Figure 2. Overall configuration of the hybrid power systems: (a) PV-diesel-battery, (b) PV-Stirling-battery.

2.4. Component specifications and inputs to HOMER

HOMER simulated various systems in order to find the one that would satisfy the user's restrictions and the lowest net present cost (NPC). It is important to highlight that an extensive literature review was carried out in order to acquire data about the local costs of the equipment used [6] [20].

PV panel parameters were introduced based on the technical characteristics of the TSM-PD14 module of TRINA SOLAR [21]. A 12 V VRLA battery (Victron Energy BAT412101104) with a nominal capacity of 110 Ah was selected [22] and two batteries per string were needed since the voltage of DC bus was assumed to be 24 V. A bi-directional inverter (which has both function of a rectifier and an inverter) did the power conditioning in the systems and was based on the Red BlueSolar 2.5 Inverter [23]. The most import parameters from diesel generator were used from the CAT C1.5 unit [24]. Finally, Stirling engine cost was based on the article presented by Swaminathan [25] that included the costs of a Stirling engine powered by biomass and its auxiliaries. The other parameters needed from the Stirling engine were based on the two alpha models, GENOA 01 (1 kW) and GENOA 03 (3 kW), both manufactured by Genoastirling [26]. Table 2 presents a summary of the systems' components characteristics as HOMER input data.

Table 2. Summary of components' specification.

Component	*Size*	*Capital cost (USD)*	*Replacement cost (USD)*	*O&M cost*	*Lifetime*
PV Panel	0.32 kW	734	344	180 (USD/year)	25 years
Battery	110 Ah	432	376	8 (USD/year)	500 cycles (80% DOD)
Bidirectional Inverter	2.5 kW	2864	2604	260 (USD/year)	15 years
Diesel Genset	1 kW	925	804	0.0124 (USD/h)	20,000 h
Stirling Engine	1 kW	4200	4200	0.0048 (USD/h)	25,000 h

Related to other parameters, the lifetime of the project was taken as 20 years, the nominal discount rate was selected as 10.10% [6], the expected inflation rate was expressed as 4.05% [27] and the annual capacity shortage was assumed to be 0%.

On the other hand, HOMER also selected the best dispatch strategy between "Cycle Charging" and "Load Following". Where "Cycle Charging" strategy refers whenever a generator is required, it operates at nominal capacity and surplus power charges the batteries [28]. Instead, in the "Load Following" strategy, when a generator is required, it produces only enough power to cover the demand [29].

The strategy for the microgrid based on the Stirling engine is limited to "Cycle Charging "; this due to the researches carried out on the use of a Stirling engine for electrification in the Bolivian rural area [30] [31]. In these works, it is explained that the "Cycle Charging" strategy is more appropriate for isolated installations since the extra energy could be used to charge the batteries. Likewise, Sugden and Drury [32], who investigated with a WhisperGen engine, stated that the "Load Following" functionality is quite slow as a result of the heat exchange process. Fig. 3 shows HOMER hybrid power systems' setup.

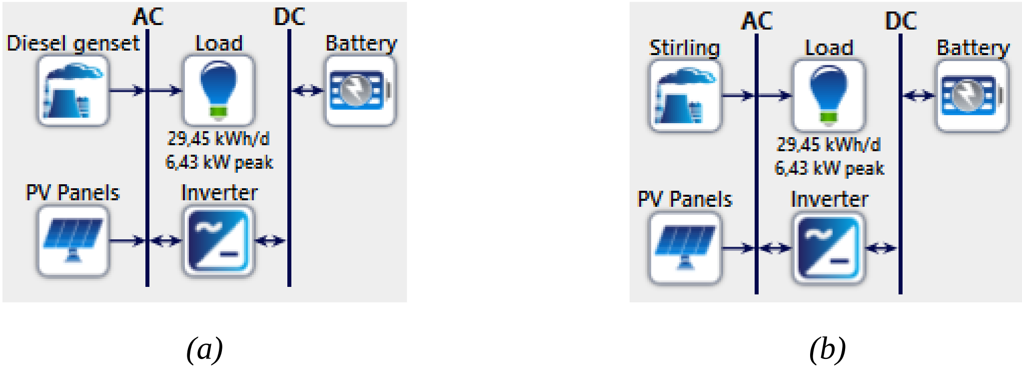

Figure 3. HOMER architecture of the hybrid power systems: (a) PV-diesel-battery, (b) PV-Stirling-battery.

3. Modelling

3.1. Photovoltaic Array

The operation of a photovoltaic cell was modelled through the equivalent circuit shown in Fig. 4. This circuit can be used to represent a single cell, a module formed by several cells or an array composed of many photovoltaic modules and is called single diode model [33].

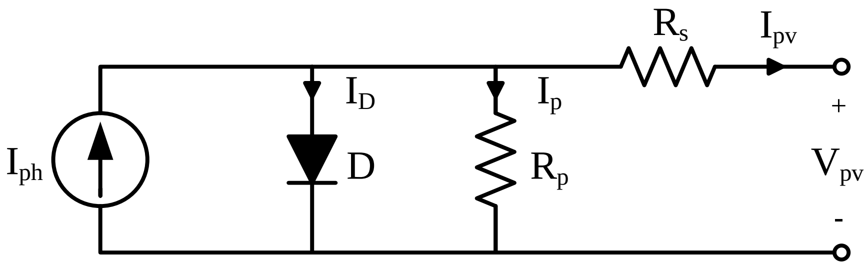

Figure 4. Equivalent circuit of PV cell: Adapted from [33].

Thus, the current at the output of the photovoltaic panel (I_{pv}) can be expressed by the relationship shown in (1) [33].

$$I_{pv} = I_{ph} - I_0 (e^{\frac{V_{pv}+I_{pv}\times R_s}{a\times N_{cel}\times V_{th}}} - 1) - \frac{V_{pv} + I_{pv} \times R_s}{R_p} \quad (1)$$

Where a is the ideality factor of the diode, I_o is the diode reverse saturation current, I_{ph} is the photoelectric current, N_{cel} is the number of cells in the module, R_s is the series resistance, R_p is the shunt resistance, V_{pv} is the voltage that exists at the output of the photovoltaic module and V_{th} is the thermal voltage of the aforementioned solar cell.

The final parameters of this model were the diode reverse saturation [34], the series resistance [35], the thermal voltage, the photoelectric current, the shunt resistance and also the cell temperature (T_{pv}) [33].

To determine the unknown parameters, an iterative method was applied based on Newton-Raphson numerical analysis [36]. Additionally, the model considers a perfect power point tracking (MPPT) controller that maximized the generated power [33].

3.1. Battery bank

The proposed model for the electrochemical battery was based on a non-linear model exposed in [37] and, at the same time, implemented in the Simulink library [38]. This makes use of a controlled voltage source in series with a constant resistance, as shown in Fig. 5.

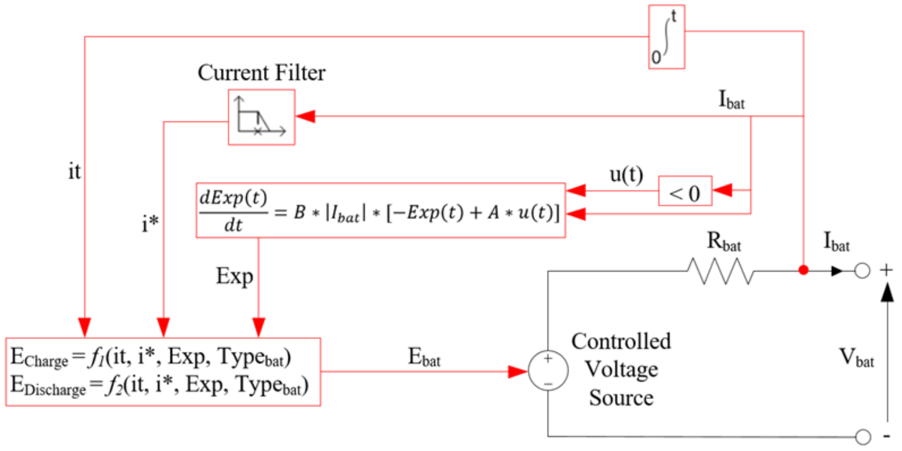

Figure 5. Non-linear model of the battery: Adapted from [37]. The black lines indicate the flow of energy and the red lines indicate the flow of information.

This model accurately represents the dynamic phenomenon of the voltage when the current varies, and the open circuit voltage is considered as a function of the state of charge of the battery [37]. Likewise, the voltage losses associated with the loading and unloading process are adequately represented and therefore, it is unnecessary to apply a constant efficiency of such processes as in other simplified models [39]. On the other hand, with this model it is possible to represent the four largest types of batteries used in electricity generation projects: Acid Lead, Lithium Ion (Li-Ion), Nickel Cadmium (NiCd) and Nickel Metal Hydride (NiMH). However, the mathematical equations vary according to the type of battery described above.

The effect of the temperature on the battery's behaviour was modelled by the adaptation made by Wijewardana [40]. Wijewardana states that the temperature influences four parameters of the battery, which are the polarization constant (K), the battery voltage constant (E_0), the exponential zone amplitude (A) and the exponential zone time constant inverse (B). However, to make the construction of a simpler model, the thermal effect on the coefficient A was ignored because the effect on A and E_0 are highly related [41].

In this way, the thermal factors that affect the three parameters are summarized in (2), (3) and (4), [40] which are shown below.

$$x_{E_0} = 0.986 + 4.97 \times 10^{-4}(T_{amb}) - 6.6 \times 10^{-4}({T_{amb}}^2) \quad (2)$$

$$x_K = 0.876 - 0.028(T_{amb}) + 4.218 \times 10^{-4}({T_{amb}}^2) \quad (3)$$

$$x_B = 0.733 - 0.055(T_{amb}) + 9.63 \times 10^{-4}({T_{amb}}^2) \quad (4)$$

Where x_{Eo}, x_K y x_B are the temperature functions for E_0, K y B respectively.

3.1. Inverter

The power balance equation through the DC/AC converter can be expressed as a function of equipment efficiency, as shown in (5) [42].

$$\eta_{inv} = \frac{P_{inv\_ac}}{P_{inv\_dc}} \tag{5}$$

Where η_{inv} represents the power converter's efficiency, P_{inv_dc} the inverter power input, and P_{inv_ac} is the inverter power output. As it can be observed, the efficiency depends on the power output of the converter and remains almost constant for output values above 0.3 p.u. [43]. In this way, in order to model this technology, the Jantsch model was used [44] and it is shown in (6).

$$\eta_{inv} = \frac{\frac{P_{inv\_ac}}{P_{inv\_nom}}}{\frac{P_{inv\_ac}}{P_{inv\_nom}} + k_0 + k_1 \frac{P_{inv\_ac}}{P_{inv\_nom}} + k_2 (\frac{P_{inv\_ac}}{P_{inv\_nom}})^2} \tag{6}$$

Where P_{inv_nom} is the nominal power of the inverter and k_0, k_1 y k_2 are constants calculated as functions of the efficiency of the converter.

3.1. Diesel generator

The diesel generator model was based on the one exposed in the article by Datta et al. [45]. This comprises of a standard model composed of a diesel engine, a speed governor and a synchronous generator. These are exemplified in Fig. 6.

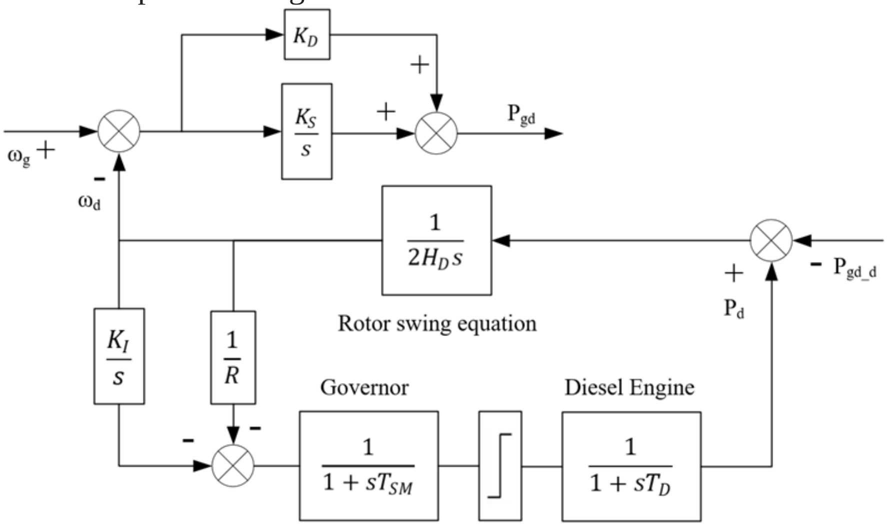

Figure 6. Block diagram of the diesel generator model. Adapted from: [45].

From Fig. 6, it can be mentioned that the diesel engine and the actuator servomechanism of the valve were represented by the first order lags, T_D and T_{SM}, respectively. Likewise, H_D is equivalent to the inertial constant of the rotor. The parameters of the speed governor were the drop (R) and integral control gain (K_I). The parameters of the synchronous generator correspond to K_S and K_D, which are the synchronization and damping coefficients, respectively. The input data were the demand (P_{gd_d}) and the velocity ω_g, corresponding to the angular velocity by another generator that can be added, for example, coming from a wind turbine (ω_g = 0 in this case). The final output data correspond to P_{gd}, the electrical power resulting from the generator.

3.1.1. Operation modes

Two modes of operation related to the diesel generator were considered (Normal and Stand-by) according to a technical publication made by the UN refugee agency [46]. Thus, a diesel genset is always in stand-by mode to be able to start immediately as a result of deficit power and during this state they have a minimum consumption by the electronic control devices.

3.1.2. Fuel consumption

The estimation of diesel consumption was based on a commonly used methodology, which is an empirical and first order polynomial equation. This approach was studied and widely disseminated by Skarstein and Uhlen [47] and is expressed in (7).

$$\dot{m}_{diesel} = k_B P_{gd\_nom} + k_A P_{gd} \tag{7}$$

Where k_A y k_B are the coefficients of consumption equation, P_{gd_nom} is the nominal capacity of the diesel genset and P_{gd} is the supplied power at a specific time.

3.1.3. Emissions

The amount of CO_2 emitted during the operation of the diesel generator was estimated as the amount of carbon in the fuel that was not converted into carbon monoxide or unburned hydrocarbons. This method is used by HOMER [48].

3.2. Stirling Engine

Regarding the modeling of the Stirling engine, an implementation was carried out based on the guidelines of Annex 42 of the International Energy Agency (IEA). This annex provides the protocol, set of tests and interrelated predictions for the modeling and validation of micro-cogeneration technologies such as internal combustion and Stirling engines, providing sufficient computer complexity to study the interaction between the cogeneration system and energy consumption on a residential building [49].
The model presented is a zero order one; in other words it does not focus on characterizing the thermodynamic behavior of the Stirling engine. Additionally, it is comprised of three control volumes: Energy conversion, thermal mass and cooling water [50]. This distribution can be seen in Fig. 7, shown below.

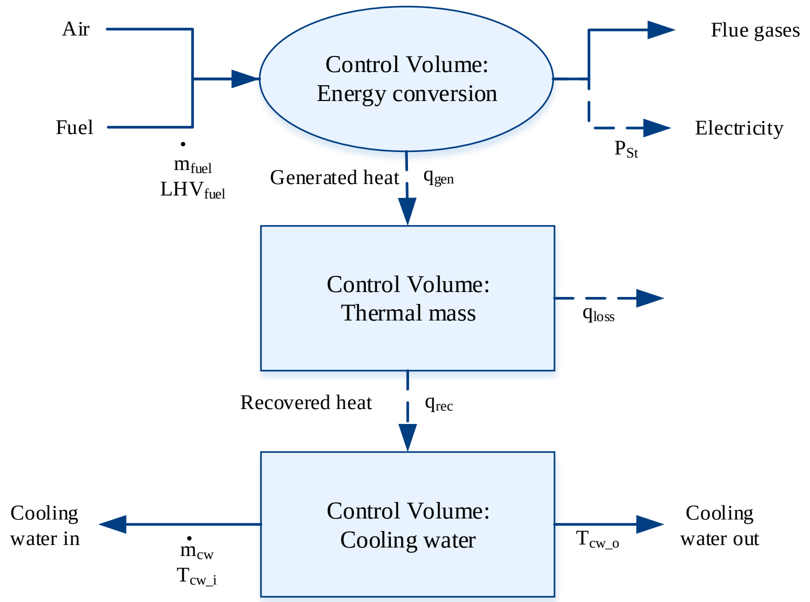

Figure 7. Mass and energy flow diagram of the Stirling engine model. Adapted from: [50].

The main reason for the selection of this model is that it has a level of intermediate complexity, allowing it to adapt to different types of fuels (natural gas and biomass) and simulate the behavior of the engine on a time scale of around one minute [51].

3.2.1. Operation modes

Besides the normal or steady operation, the cogeneration unit based on a Stirling engine can operate in three other modes, which are stand-by, warm-up and cool-down. During warm-up, the engine generates a partial amount of electrical and thermal power. Under cool-down and stand-by modes, the device does not generate electricity or heat, but consumes electrical power to maintain activation functions or to complete the shutdown [50].

3.2.2. Fuel consumption

The biomass consumption was estimated using the same equation from the diesel genset, shown in (7), but the coefficients were calculated with the electrical efficiency of the Stirling engine and the data from Lane and Beale's investigation [52].

3.2.3. Emissions

The CO_2 emissions were calculated with the data expressed by Harrison for a Stirling engine working in a cogeneration unit [53].

3.2. Control Strategy

A control algorithm was developed. This determined the interaction between different components of the system, specifically establishing the start-up and shut-down of the generator (Stirling engine or diesel generator), the operation of the battery, the introduction or curtailment of the photovoltaic system. Consequently, an appropriate control strategy increases the availability of electrical energy, system efficiency, battery life, and amount of electrical power generated [54]." Load Following-Frugal" strategy for the PV-diesel-battery system and "Cycle Charging-Frugal-SOC Setpoint" strategy for PV-Stirling-battery system were studied in this work.

3.3.1. Load Following-Frugal Strategy

This dispatch strategy combines two dispatch strategies. Assuming that the operation of "Load Following" strategy is based on the supply power of the generator, this will only give what is required, hence supplying a balanced demand without providing unnecessary energy to batteries' charge. On the other hand, "Frugal strategy" considers a critical discharge power (L_d) overcoming the net power, the cost of energy generation with the generator is less than covering that energy with the batteries. That is, the generator will supply the net load whenever this is greater than the value of Ld, whether the batteries can cover that electrical demand or not [55]. Fig. 8 exemplifies both combined strategies.

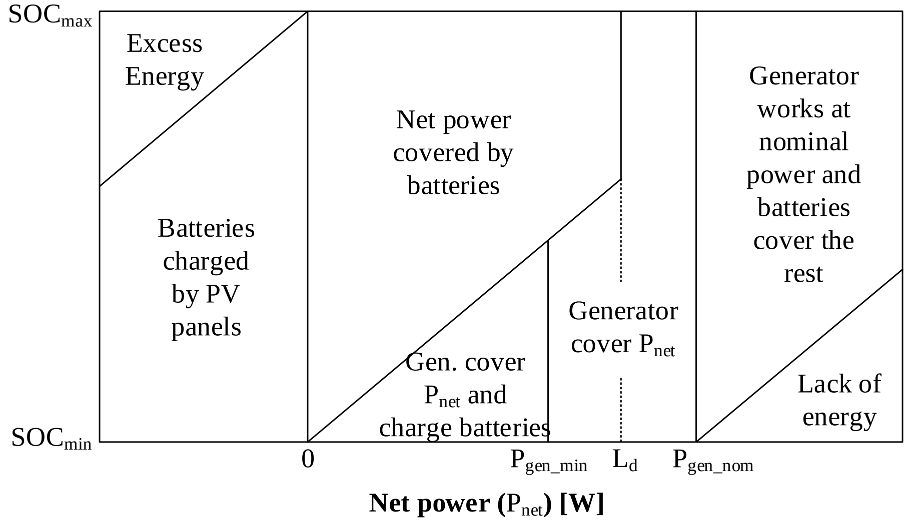

Figure 8. Simplified diagram of "Load Following-Frugal" strategy.

The basic principle of the combined strategy is to use the photovoltaic source in order to supply the electrical power demand. Thus, the net power (P_{net}) is defined as the subtraction between the power produced on the solar models and the demand of power (P_d). Thus, if there is an excess of power generated by PV modules ($P_{net} > 0$), then this will be used to charge the batteries. However, prior evaluation, the actual state of charge of the batteries should be revised (SOC) since there is a minimum value (SOC_{min}) and a maximum value (SOC_{max}) of work allowed. Also, there are certain limits of charge (P_{max_car}) and discharge rates (P_{max_des}). Therefore, all limits of battery charging and discharging conditions must be respected. In case the batteries are already fully charged, the excess power is discharged or discarded (P_{exc}). In another case, if the net power is negative ($P_{net} < 0$), the first step is to evaluate if the net power is less than L_d, as well as to revise if the SOC of the batteries is greater than the minimum SOC; then the batteries can supply part of the demand until they reach their maximum discharge rate (P_{max_des}). On the other hand, if the net power required is greater than or equal to L_d, or the current SOC of the batteries has a low value, the possibility of starting the generator is examined, since it also has a working limit (30% of the power rated diesel generator in this analysis), this will secure efficient operation and a longer life time. So, in case the net power is lower than the working limit of the generator this will be activated, and the excess energy will be used to charge the batteries, respecting their limits. In any other situation, the batteries are not charged by the generator, unless their generated power is higher than the net power. As a last option, if all the technologies are not able to cover the demand power, there is a type of electrical energy not supplied (P_{def}).

3.3.1. Cycle Charging-Frugal-SOC Setpoint Strategy

The operation of this strategy combines three different ones (Fig. 9). “Cycle Charging” strategy differs from the “Load Following” one, when the batteries are unable to cover the net power, the generator will operate at nominal power charging the batteries with the remaining power. On the other hand, the SOC Setpoint implies that the generator will continue to operate until the batteries reach a state of charge corresponding to SOCstp.

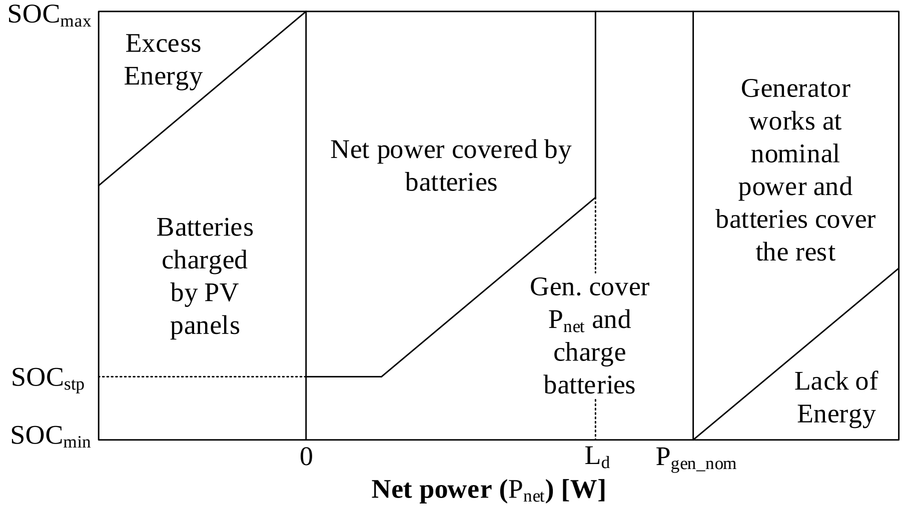

Figure 9. Simplified diagram of “Cycle Charging-Frugal-SOC Setpoint” strategy.

4. Performance analysis

Both systems are evaluated in terms of energy, economic and environment using Fuel Saving Ratio (FSR), Annualized Total Cost Saving Ratio (ATCSR) and CO2 Emission Reduction Ratio (CO2ERR) respectively.

4.1. Energy efficiency evaluation

Fuel Saving Ratio (FSR) represents a measure used to compare the equivalent energy of the fuel consumption of the studied system in relation to the reference system and can be calculated through (8) [13].

$$FSR = \left(1 - \frac{F_{sis\_tot}}{F_{ref\_tot}}\right) 100\% \quad (8)$$

Where F_{sis_tot} y F_{ref_tot} are the equivalent energy of the fuel consumption by the studied system and by the referential system respectively.

4.2. Economic feasibility evaluation

Regarding the economic comparison of the studied system with the referential system, the Annualized Total Cost Saving Ratio (ATCSR) is used. This is a measure calculated with (9) [13].

$$ATCSR = \left(1 - \frac{ATC_{sis\_tot}}{ATC_{ref\_tot}}\right) 100\% \quad (9)$$

Where ATC_{sis_tot} y ATC_{ref_tot} are the annualized total costs of the system under study and the reference system respectively. On the other hand, the total annualized cost (ATC) includes all costs during the lifetime of the project.

4.3. Environmental sustainability evaluation

The CO_2 emission reduction ratio (CO2ERR) is constituted in the environmental index. The value of this factor is known as the relation between the CO_2 emissions during the operation of the studied system ($CO2_{sis\_tot}$) and the CO2 emissions of the reference system ($CO2_{ref\_tot}$). Equation (10) shows this trend.

$$CO2ERR = \left(1 - \frac{CO2_{sis\_tot}}{CO2_{ref\_tot}}\right) 100\% \quad (10)$$

4.4. Weighting factor method

The three criteria of performance analysis can be integrated into a weighted factor method to formulate an integrated saving ratio (IRS), which is defined in (11).

$$ISR = w_1 \cdot FSR + w_2 \cdot CO2ERR + w_3 \cdot ATCSR \quad (11)$$

Where, w_1, w_2 y w_3 represent the weighted factors of each criterion. These factors had equal values (1/3). This is an assumption that had been made in several studies of the energy field [56] [57] [58].

5. Results and discussion

5.1. Homer Sizing

HOMER results expressed that PV-Stirling-battery system would be composed of a 5.45 kW solar array, a 6 kW Stirling engine, a 6.92 kW bi-directional inverter and a 71.28 kWh VRLA gel lead-acid battery bank. The second system would be comprised of 3.95 kW PV panels, a 7.1 kW diesel generator, a 4.46 kW bi-directional inverter and a 50.16 kWh VRLA gel lead-acid battery bank.

5.2. Dynamic Analysis

As it was previously mentioned, first a simulation for a representative solar radiation day was made (winter solstice) and then, this was followed by an annual simulation of the systems.

For the winter solstice (June 21st), as shown in Fig. 10.a, the electrical generation by PV modules occurs around 7:00 am to 6:00 pm. Furthermore, the supply by this technology is intermittent and its peak is reached around noon. On the contrary, the diesel generator only works during the period of high electrical demand (approximately from 19:00 to 22:00), because the value of critical discharge power (L_d) registers a value of 4392.15 W. In another aspect, peaks of the battery charging and discharging power, during operation of the diesel engine can also be observed. These last around 30 seconds, which is the time that the diesel generator takes to start-up and stabilize at the required power. In case there is a day with low solar radiation, the batteries can cover the electricity demand, and therefore no period of energy deficit nor an excess of energy will occur, as exemplified in Fig.10.b. It is worth mentioning that at the end of the day the battery ends up in a state of charge of 40% (Fig. 10.c), close to its 30% limit.

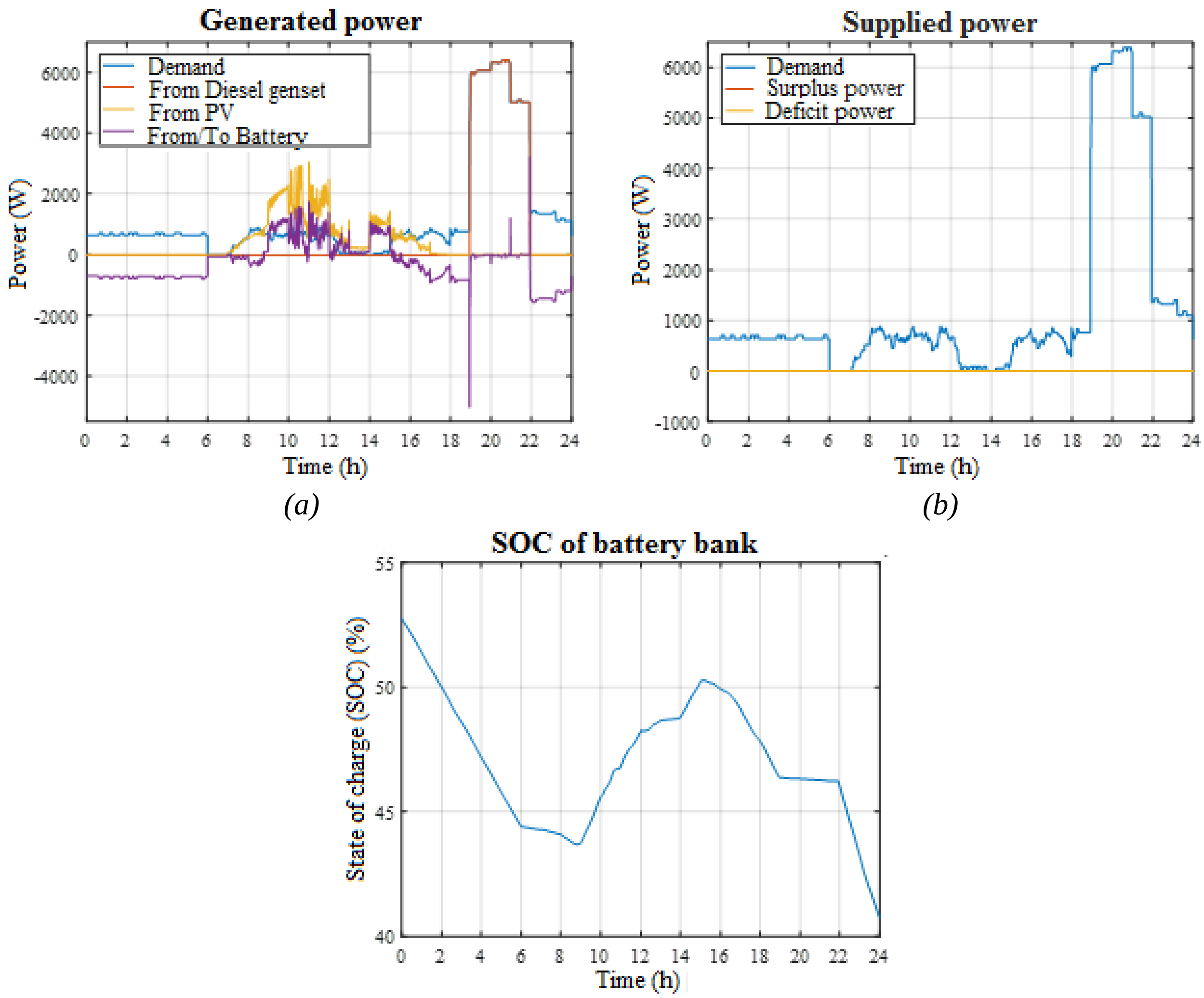

(a) *(b)* *(c)*

Figure 10. Results of the simulation of the PV-Diesel-battery system for (a) Generated power, (b) Supplied power and (c) State of charge of the battery bank during June 21st.

In comparison, during the winter solstice by the PV-Stirling-battery system, it is possible to observe that after the Stirling engine starts (around 19:00), it keeps running until the battery bank reaches its set point around 9:00 p.m. (Figs 11.a to 11.c). The electricity demand shown in Fig. 11.b, is completely covered in this scenario. The simulation of this hybrid power system required adding a SOC setpoint for the battery because after the battery reached the minimum state of charge in a "Load Following-Frugal" strategy, it reflected an intermittent behavior while the demand was less than the Ld value. However, the extra time that the Stirling engine works in the "Load Following-Frugal-SOC setpoint" strategy, it incurs in a higher fuel consumption and higher emissions released compared to the operation of the PV-diesel-battery system under the same conditions on the winter solstice.

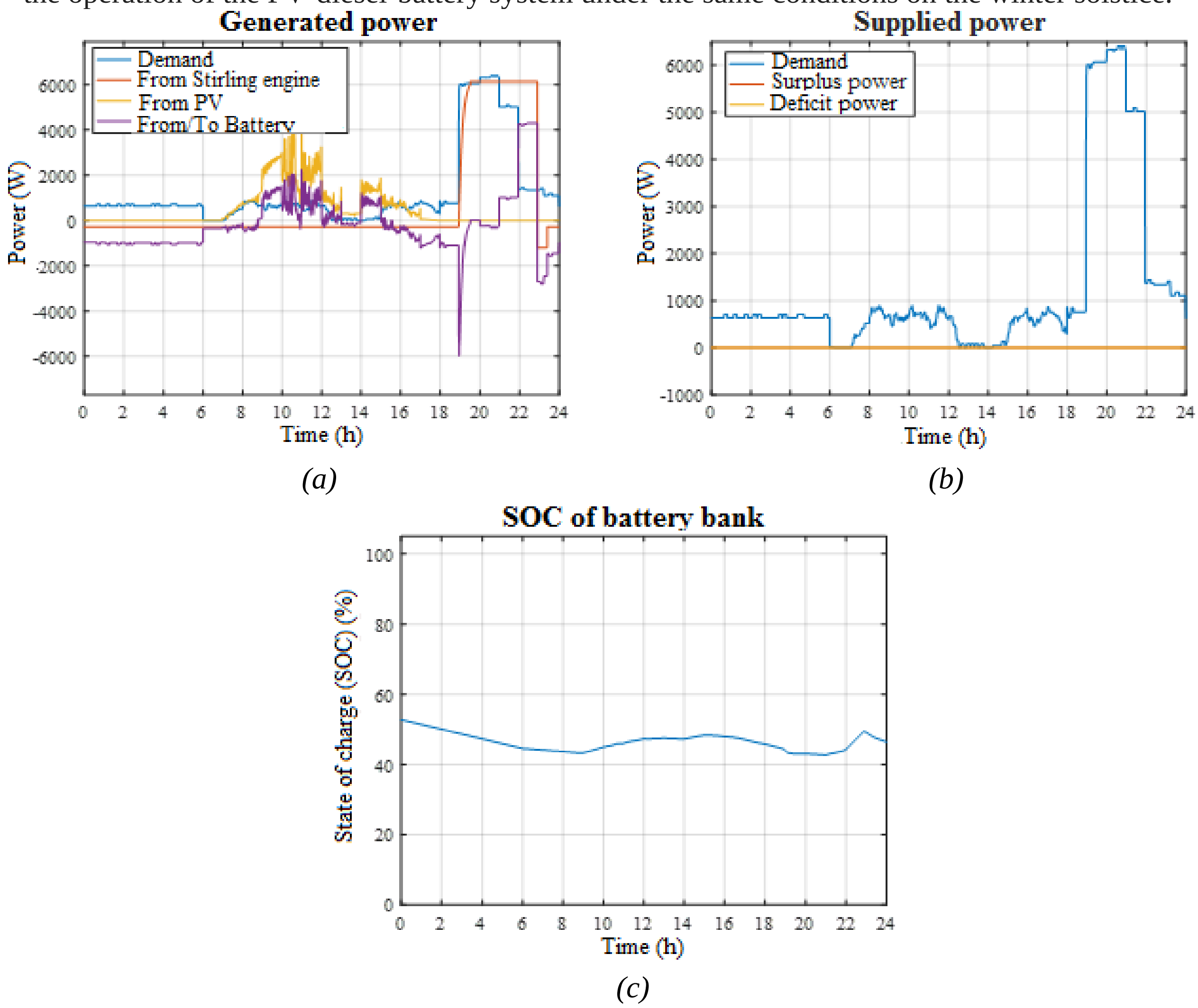

Figure 11. Results of the simulation of the PV-Stirling-battery system for (a) Generated power, (b) Supplied power and (c) State of charge of the battery bank during June 21st.

5.3 Performance Analysis

The evaluation of the performance of the hybrid generation systems was carried out in terms of Fuel Saving Ratio (FSR), carbon dioxide emission reduction ratio (CO2ERR), Annualized Total Cost Saving Ratio (ATCSR) and Integrated Saving ratio (IRS), compared to a traditional rural electrification project based on diesel generation. These results are shown in Table 2.

Table 2. Results of the annual performance evaluation of the hybrid systems PV-diesel-battery system and PV-Stirling-battery system.

Rate [%]	*PV-diesel-battery system*	*PV-Stirling-battery system*
FSR	70	41
CO2ERR	70	73
ATCSR	32	0
ISR	57	38

As shown in the previous table, both hybrid systems present energy, economic and environmental benefits compared to a traditional generation system. However, the value of the integrated saving ratio (ISR) is much higher for the PV-diesel-battery system. The fuel saving ratio for the aforementioned micro-grid is 70%. This result is similar to the design value of the same hybrid system at another community ("Río Apere") in Beni, where a 63% reduction in diesel consumption is mentioned [59]. Likewise, a performance study of the PV-diesel-battery microgrid in the city of Sabah of Malaysia, which has climatic characteristics similar to the community of Tacuaral de Mattos, specifies a reduction of up to 80% of diesel consumed annually [60]. Regarding the CO2ERR ratio, we can verify that the value of 70% of CO2 emissions reduction is similar to the reduced emissions rate in the city of Sabah, which is 80% [60].

On the other hand, the PV-Stirling-battery system owns an FSR ratio of only 41%. This is the result of low electrical efficiency and higher pellet consumption due to the strategy based on the SOC Setpoint.

Also, the aforementioned system is much more expensive than the traditional one, and therefore, the savings ratio of the annualized total cost is zero. However, the PV-Stirling-battery system can reduce 3% more carbon dioxide emissions compared to the system based purely on diesel (10% of reduced emissions compared to the PV-diesel-battery system). Unfortunately, there are no studies regarding the performance of PV-Stirling-battery system that works in isolated mode and utilizes biomass as fuel. However, there are two studies of cogeneration systems based on the Stirling engine. The first refers to the analysis of residential cogeneration systems, including two Stirling engines, (WhisperGen and Solo), compared to a gas combined cycle power plant [61]. While the second research is focused on the performance of a residential cogeneration system based on a natural gas Stirling engine, photovoltaic modules, thermal storage and refrigeration equipment [62]. Both studies are based on different technologies and scenarios. Therefore, they do not have sufficient scientific validity to be compared with the simulation of the PV-Stirling-battery system presented in this thesis, and therefore, only the comparison is related to the formulated PV-diesel- battery system.

6. Conclusions

The following research carried out an economic optimization that presented the dimensions of the technologies that composed the PV-diesel-battery and PV-Stirling-battery systems, considering the electricity demand of the rural community from Beni, "Tacuaral de Mattos". Thus, this first part of the study revealed a big economic difference between both hybrid systems; as a result of the high purchase price of the Stirling engine (4200 USD/kW), and due to the fact of its unavailability in the Bolivian market.

Subsequently, dynamic models were developed for each component using numerical methods present in the selected software. Each model considers different specific factors to each technology and, also, the effect of temperature. On the other hand, the model of the generators determines the emissions produced and the fuel consumption during its operation. Thus, these models have sufficient flexibility to become tools that can be used in other studies in the field.

The dispatch strategies designed allowed an economic operation of the systems, when considering a critical power value of battery discharge, and stable operation, in terms of energy deficit and preserving the useful life of all the components. For this purpose and in order to avoid thermal stress by the Stirling engine, a fixed-point strategy of the battery's charge status was included.

The integration of the systems was carried out through a simulation of a full day considering a representative solar day (Winter solstice). This integration showed a certain trend of lower fuel consumption by the PV-diesel-battery system and a lower amount of emissions by the PV-Stirling-Battery system. It is worth mentioning that the approximate time of the mentioned simulation was 45 seconds.

Finally, the performance of the studied systems were evaluated successfully, by using an indicator based on a weighting of the energy, economic and environmental factors. For this study, the hybrid system based on a diesel generator, PV modules and batteries represented, in a weighted analysis, a better option to implement in a rural electrification project compared to a system made up of Stirling engine, PV modules and batteries. However, the latter showed a better environmental sustainability, being able to reduce carbon dioxide emissions during its operation. It is also important to note that the time of the annual simulation for the performance analysis was 3 and a half hours.

In summary, more research is required before a hybrid power system based of diesel generation becomes obsolete. However, there is a great opportunity for systems based on Stirling engines to benefit users of distributed energy systems, as the technology matures, and more developments are made in the energy field.

7. References

[1] H. Khatib, "Electricity in the global energy scene," *IEE Proceedings A (Science, Measurement and Technology)*, no. 140, pp. 24-28, 1993.

[2] International Energy Agency [IEA], Energy Access Outlook 2017, World Energy Outlook 2017 Special Report, 2017.

[3] A. Agrawal, R. Wies and R. Johnson, Hybrid Electric Power Systems: Modeling, Optimization and Control, AV Akademikerverlag, 2012.

[4] S. Balderrama, W. Canedo, V. Lemort and S. Quoilin, "Techno-economic optimization of isolate micro-grids including PV and Li-Ion Batteries in the Bolivian context," in *Proceedings of ECOS 2016 - the 29th International Conference on Efficiency, Cost, Optimization, Simulation and Environmental Impact of Energy Systems*, 2016.

[5] Autoridad de Fiscalización y Control Social de Electricidad [AE], "Anuario Estadístico 2017," 2018.

[6] Banco Interamericano de Desarrollo [BID], "Evaluación Financiera y Económica del Proyecto Electrificación Rural con Energía Renovable (BO-X1013)," Cochabamba, Bolivia, 2013.

[7] ENDE Guaracachi, "Planta solar fotovoltaica Cobija," 2015. [Online]. Available: http://guaracachi.com.bo/index.php?option=com_content&view=article&id=48&Itemid=251. [Accessed 4 Octubre 2017].

[8] Ministerio de Comunicación, "Gobierno lleva energía eléctrica a comunidad guaraní 'El Espino'," 22 Octrubre 2015. [Online]. Available: http://www.comunicacion.gob.bo/?q=20151022/19658. [Accessed 25 Octubre 2016].

[9] Meteonorm, "Meteonorm Features," 1 Agosto 2017. [Online]. Available: http://www.meteonorm.com/en/features/features. [Accessed 29 Agosto 2017].

[10] S. Mandelli, E. Colombo and M. Merlo, "Novel procedure to formulate load profiles for off-grid rural areas," *Energy for Sustainable Development*, no. 31, pp. 130-142, 2016.

[11] HOMER Energy, "HOMER v. 3.10.1," USA, 2017.

[12] Mathworks, “MatLab & Simulink: Simulink Reference R201a,” [Online]. Available: https://www.mathworks.com/help/simulink/release-notes-R2017a.html. [Accessed 15 Diciembre 2017].

[13] S. Ghaem Sigarchian, A. Malmquist and V. Martin, “Optimal planning and design method for complex polygeneration systems: A case study for a residential building in Italy,” *Energy Convers Manage,* 2018.

[14] Instituto Nacional de Estadística [INE], “Censo Nacional de Población y Vivienda,” 2012.

[15] M. Lucano and I. Fuentes, “Evaluación del potencial de radiacion solar global en el departamento de Cochabamba utilizando modelos de sistemas de información geográficas e imágenes satelitales,” *Revista Boliviana de Física,* no. 17, pp. 13-21, 2010.

[16] M. Hallberg and E. Hallme, “Energy demand in different topographical zones,” Bachelor thesis in Energy and Environment, Estocolmo, 2015.

[17] S. Balderrama, A. Tarantino, S. Sabatini, F. Riva, G. Bonamini and S. Quoilin, “Feasibility Study of PV & Li-Ion Battery Based Micro-Grids for Bolivian Off-Grid Communities,” *Proceedings of IRES 2017 - The 11th International Renewable Energy Storage Conference,* 2016.

[18] E. Toledo and J. L. Arteaga, “Proyecto de electrificación rural "Central Caranavi",” Gobierno Municipal de Caranavi, La Paz, 2008.

[19] ENERSOL, “ENERSOL-Soluciones Globales de Energía,” 2017. [Online]. Available: http://www.enersol-sa.com/proyecto-fotovoltaico-el-espino. [Accessed 10 Noviembre 2016].

[20] Enersol S.A., “Tienda,” [Online]. Available: http://tienda.enersol-sa.com/. [Accessed 2 February 2018].

[21] TRINA SOLAR, “Hoja técnica del modelo TSM-PD14,” Noviembre 2017. [Online]. Available: http://www.enersol-sa.com/images/stories/Descarga-hoja-tecnica/energia-solar/paneles-solares/Trina-solar/es_hoja_tecnica_b_310-325W.pdf. [Accessed 22 Noviembre 2017].

[22] Victron Energy, “Catálogo de baterías Gel y AGM,” Holanda, 2017.

[23] Victron Energy, “Invesor Red BlueSolar,” 2015. [Online]. Available: https://www.victronenergy.com.es/upload/documents/Datasheet%20-%20BlueSolar%20Grid%20Inverter%20-%20rev%2005%20-%20ES.pdf. [Accessed 12 Diciembre 2017].

[24] Caterpillar Inc., “Datos técnicos y precio del grupo electrógeno C2.2,” Finning CAT, 2016. [Online]. Available: http://www.finning.com/es_BO/products/new/power-systems/electric-power-generation/diesel-generator-sets/1000001191.html. [Accessed 22 Noviembre 2017].

[25] R. Swaminathan, “Cost Effective, Low Capacity, Biomass Fired Power Plant,” *Energy and Power,* no. 3, pp. 1-6, 2013.

[26] Genoastirling S.R.L, “GENOA STIRLING,” 20 Diciembre 2017. [Online]. Available: https://genoastirling.com/attach/Catalogo_2017_ENG.pdf. [Accessed 10 Enero 2018].

[27] Banco Central de Bolivia [BCB], “Indicadores de Inflación Anual,” 22 Noviembre 2017. [Online]. Available: https://www.bcb.gob.bo/?q=indicadores_inflacion. [Accessed 22 Noviembre 2017].

[28] HOMER Energy, “Cycle Charging,” 2017. [Online]. Available: https://www.homerenergy.com/support/docs/3.11/cycle_charging.html. [Accessed 10 Diciembre 2017].

[29] HOMER Energy, “Load Following,” Agosto 2017. [Online]. Available: https://www.homerenergy.com/support/docs/3.11/load_following.html. [Accessed 20 Diciembre 2017].

[30] J. Arco Sola and O. Nelson, “Applications of biomass Stirling Engine for electrification. A case study of rural areas in Bolivia.,” Tesis de Licenciatura, Real Instituto de Tecnología (KTH), Estocolmo, 2014.

[31] H. Ljunggren Falk and S. Berg, “Implementation of a Stirling engine generation system for residential use in rural areas of Beni department of Bolivia,” Tesis de Licenciatura, Real Instituto de Tecnología (KTH), Estocolmo, 2014.

[32] B. Sugden and T. Drury, “Investigation into the viability of replacing internal combustion diesel generators with diesel fired stirling engine generators for remote microwave radio telecommunication applications,” *2012 IEEE International Telecommunications Energy Conference,* pp. 1-8, 2012.

[33] J. Duffie and W. Beckman, Solar Engineering of Thermal Processes, Cuarta ed., Nueva York: John Wiley & Sons Inc., 2013.

[34] M. Villalva, J. Gazoli and E. Filho, “Comprehensive approach to modeling and simulation of photovoltaic arrays,” *IEEE Transactions on Power Electronics,* no. 24, pp. 1198-1208, 2009.

[35] A. Virtuani, E. Lotter and M. Powalla, “Performance of Cu (In,Ga) Se solar cells under low irradiance,” *Thin Solid Films,* pp. 443-447, 2003.

[36] V. V. Ramana and D. Jena, “An Accurate Modeling of Photovoltaic System for Uniform and Non-Uniform Irradiance,” *International Journal of Renewable Energy Research,* no. 5, 2015.

[37] O. Tremblay and L. A. Dessaint, “Experimental Validation of a Battery Dynamic Model for EV Applications,” *Experimental Validation of a Battery Dynamic Model for EV Applications,* no. 3, pp. 40-49, 2009.

[38] MathWorks, “Documentation: Implement generic battery model,” Enero 2018. [Online]. Available: https://www.mathworks.com/help/physmod/sps/powersys/ref/battery.html. [Accessed 10 Julio 2018].

[39] N. DiOrio, A. Dobos, S. Janzou, A. Nelson and B. Lundstrom, “Technoeconomic Modeling of Battery Energy Storage in SAM,” Rporte de Laboratorio Nacional de Energías Renovables de Estados Unidos, 2015.

[40] S. Wijewardana, “New Dynamic Battery Model for Hybrid Vehicles and Dynamic Model Analysis Using Simulink,” *Journal of the Institution of Engineers,* vol. 47, no. 04, p. 53–61, 2014.

[41] Y. Tan, J. Mao and K. Tseng, “Modelling of battery temperature effect on electrical characteristics of Li-ion battery in hybrid electric vehicle,” in *IEEE 2011 IEEE Ninth International Conference on Power Electronics and Drive Systems (PEDS 2011),* Singapore, 2011.

[42] G. Rampinelli, A. Krenzinger and F. Chenlo Romero, “Mathematical models for efficiency of inverters used in grid connected photovoltaic systems,” *Renewable and Sustainable Energy Reviews,* vol. 34, pp. 578-587, 2014.

[43] L. Monteiro, I. Finelli, A. Quinan, W. Macedo, P. Torres and J. T. Pinho, “Implementation and validation of energy conversion efficiency inverter models for small pv systems in the north of Brazil,” *Renewable Energy in the Service of Mankind,* vol. II, pp. 93-102, 2016.

[44] R. Tapia, C. R. Fuerte Esquivel, E. Espinosa Juarez and U. Sandoval, “Steady-state model of grid-connected photovoltaic generation for power flow analysis,” *IEEE Transactions on Power Systems,* pp. 1-10, 2018.

[45] M. Datta, T. Senjyu, A. Yona, T. Funabashi and C.-H. Kim, “A Frequency-Control Approach by Photovoltaic Generator in a PV–Diesel Hybrid Power System,” *IEEE Transactions on Energy Conversion,* vol. 26, pp. 559-571, 2011.

[46] Agencia de la ONU para los Refugiados, “Diesel Generators: Technical Specification,” 2017.

[47] O. Skarstein and K. Uhlen, “Design considerations with respect to long-term diesel saving in,” *Wind Engineering,* vol. 13, pp. 72-87, 1989.

[48] HOMER Energy, “How HOMER Calculates Emissions,” Enero 2018. [Online]. Available: https://www.homerenergy.com/products/pro/docs/3.11/how_homer_calculates_emissions.html. [Accessed 1 Julio 2018].

[49] I. Beausoleil-Morrison, “An Experimental and Simulation-Based Investigation of the Performance of Small-Scale Fuel Cell and Combustion-Based Cogeneration Devices Serving Residential Buildings,” IEA/ECBCS Annex 42 Final Report, Canadá, 2008.

[50] A. Ferguson, N. Kelly, A. Weber and B. Griffith, “Modelling residential-scale combustion-based cogeneration in building simulation,” *Journal of Building Performance Simulation,* vol. 2, pp. 1-14, 2009.

[51] J.-B. Bouvenot, “ Etude expérimentales et numériques de systèmes de micro cogénération couplés aux batiments d'habitation et au réseau électrique,” Tesis doctoral, Universidad de Strasbourg, 2015.

[52] N. Lane and W. Beale, “A Biomass-Fired 1 kWe Stirling engine generator and its applications in South Africa,” *9th International Stirling Engine Conference,* 1999.

[53] J. Harrison, “Stirling engine systems for small and micro combined heat and power (CHP) applications,” in *Small and micro combined heat and power (CHP) systems*, Inglaterra, Woodhead Publishing Limited, 2011, p. 183.

[54] C. Barley, C. Winn, L. Flowers and H. Green, “Optimal control of remote hybrid power systems, Part,” *WindPower95,* 1995.

[55] R. Dufo López and J. L. Bernal-Agustín, Generación de Energía Eléctrica con Fuentes Renovables: Optimización de Sistemas Híbridos Renovables con Almacenamiento Energético Mediante Algoritmos Genéticos, Zaragoza: Editorial Académica Española, 2011.

[56] J. Wang, Z. Zhai, Y. Jing and C. Zhang, “Particle swarm optimization for redundant building cooling heating and power system,” *Applied Energy,* vol. 87, p. 3668–3679, 2010.

[57] L. Li, H. Mu, W. Gao and M. Li, “Optimization and analysis of CCHP system based on energy loads coupling of residential and office buildings,” *Applied Energy,* pp. 206-216, 2014.

[58] C. Zheng, J. Wu and X. Zhai, “A novel operation strategy for CCHP systems based on minimum distance,” *Applied Energy,* vol. 128, pp. 25-35, 2014.

[59] N. Bellot Rodriguez, “Diseño de un Sistema híbrido fotovoltaico-diésel en la localidad del "Perú del Río de Apere" en el departamento de Beni,” Proyecto de Grado de Licenciatura en Ingeniería Eléctrica, Cochabamba, 2013.

[60] L. .. Halabi, S. Mekhilef, L. Olatomiwa and J. Hazelton, “Performance analysis of hybrid PV/diesel/battery system using HOMER: A case study Sabah, Malaysia,” *Energy Conversion and Management,* vol. 144, pp. 322-339, 2017.

[61] P. Michel De Paepe and D. M. D'Herdt, "Micro-CHP systems for residential applications," *Energy Conversion and Management*, vol. 47, pp. 3435-3446, 2006.

[62] C. Brandoni and M. Renzi, "Optimal sizing of hybrid solar micro-CHP systems for the household sector," *Applied Thermal Engineering*, vol. 75, pp. 896-907, 2015.